Integrated Optical Circulator based on Radiatively Coupled Magnetooptic Waveguides

M. Lohmeyer, M. Shamonin, P. Hertel
Department of Physics, University of Osnabrück,
Barbarastraße 7, D-49069 Osnabrück, Germany

Abstract: In a three-guide coupler with multimode central waveguide more than two modes of the entire structure participate in the coupling between the outer waveguides. Using a three mode approximation we found simple conditions for complete power transfer between the outer waveguides: the device length has to match certain multiples of the conventionally defined coupling length. The specific form of the relevant modes allows to design a magnetooptic isolator or circulator with significantly reduced device length (as compared to the conventional nonreciprocal coupler). The performance of the proposed devices is simulated by propagating mode calculations. Estimates for admissible fabrication tolerances for the layer thicknesses are presented.

Keywords: integrated optics, radiatively coupled waveguides, three-guide coupler, magnetooptic isolator, magnetooptic circulator

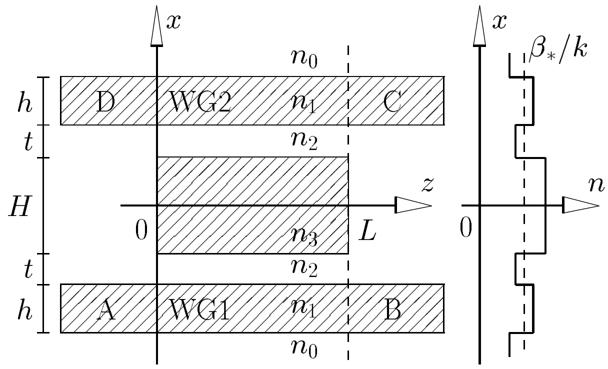

Figure 1: Geometry of planar radiatively coupled waveguides. The central layer (thickness H, refractive index n_3) couples the two identical outer waveguides WG1 and WG2 (thickness h, refractive index n_1). The outer layers are separated from the central layer by a slab of thickness t and refractive index n_2. The structure is embedded within a medium of refractive index n_0.

1 Introduction

Magnetic garnets are promising materials for the realization of nonreciprocal integrated optical components (such as isolators and circulators) in the near infrared [1, 2]. Unfortunately, thin garnet films also show undesirably high optical losses [3]. For the available materials with their limited Faraday rotation design concepts have to be developed which aim at very short device lengths.

Recent proposals are based on the nonreciprocal phase shift in magnetooptic waveguides [4, 5, 6]. In a nonreciprocal coupler, the difference of the mode interference patterns in forward and backward directions is used for separating the counterpropagating waves. The main problem of this concept is the requirement to have strongly coupled, but spatially well separated optical channels. Recently we proposed to use a three-waveguide coupler (so-called radiatively coupled waveguides) to overcome this dilemma [7]. In this paper we investigate such a system in detail, focusing at the regime where mainly three modes participate in the coupling process. We show that it is possible to design an integrated optical circulator with remarkable characteristics.

Three-guide structures have been investigated by means of coupled mode theory [8], as a system of two leaky waveguides [9, 10], or as multilayered waveguides [11, 12, 13]. This work is based on the latter approach. Depending on the thickness of the central waveguide, mainly two or three modes determine the coupling between the outer waveguides. As for the conventional two-waveguide coupler, a characteristic coupling length can be defined. The power transferred between the outer waveguides exhibits maxima and minima if the device length is chosen as a multiple of the coupling length provided that additional conditions on the propagation constants are satisfied.

These considerations are presented in section 2. In section 3 the concept of the nonreciprocal coupler [14] is applied to radiatively coupled waveguides. The special form of the relevant modes can be used for an optimization of the nonreciprocal phase shift to obtain a small device length. In particular, the case with three relevant modes turns out to be interesting. Section 4 reports on numerical calculations, section 5 contains some remarks for a realization in rib waveguide form .

2 Three-guide coupler with multimode central waveguide

Fig. 1 shows a cross section of the planar structures discussed in this paper. Each of the two identical outer waveguides supports only one mode with propagation constant β_*, for given vacuum wavelength $\lambda = 2\pi/k$ and polarization state (TE or TM). To achieve remote coupling between the outer waveguides, n_3 must be larger than the effective index β_*/k. Then the propagation constants β of the entire structure typically exhibit a nearly periodic dependence on the thickness H of the central waveguide as depicted in Fig. 2.

Assume that the structure with thickness $H = H_0$ supports a mode with propagation constant β. In

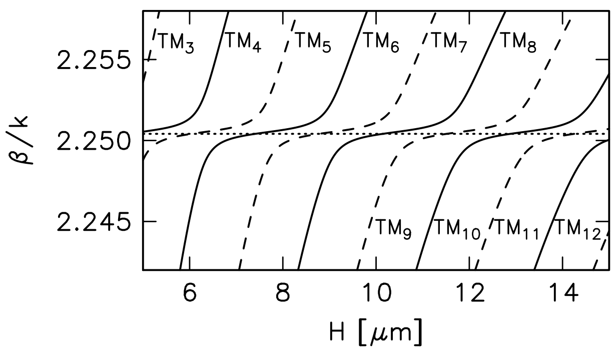

Figure 2: Effective mode indices for TM-polarized modes versus the thickness of the central layer. Remaining parameters are: $\lambda = 1.3\mu$m, $n_0 = n_2 = 2.18$, $n_1 = n_3 = 2.30$, $h = 0.8\mu$m, $t = 0.8\mu$m. Only a small fraction of the region allowed for the mode indices is displayed. Symmetric modes are indicated by continuous lines, antisymmetric modes by dashed lines. The dotted line shows the level $\beta^*/k = 2.25041$.

the central layer the mode function varies sinusoidally along the x coordinate with a spatial period of $2\pi/\sqrt{k^2 n_3^2 - \beta^2}$. Therefore, modes with the same propagation constant β exist in a set of waveguides with thicknesses $H_j = H_0 + j\pi/\sqrt{k^2 n_3^2 - \beta^2}$ ($j = 1, 2, \ldots$), too. These modes are symmetric (even j) or antisymmetric (odd j) with respect to the reflection $x \to -x$. The shape of the mode function remains unchanged apart from the sine or cosine term inserted at $H_j - H_0$.

For each thickness H there are either two or three propagation constants close to β_*. The corresponding modes contribute with large amplitudes to light propagation if the structure is excited by the guided mode of one outer waveguide. In some cases the coupling behaviour may be well characterized by the interference of only three modes. Fig. 3 shows the corresponding mode functions and their superposition.

Let us now discuss the coupling of power between the two outer waveguides. Denote by χ_j the normalized (guided) mode functions of the entire structure: $\langle \chi_k, \chi_j \rangle = \delta_{kj}$. β_j are the corresponding propagation constants. The scalar product for TM modes is $\langle \phi, \chi \rangle = \int n(x)^{-2} \phi^*(x) \chi(x)\, dx$, the inverse permittivity being absent for TE modes. For sufficiently large gap width t (cf. Fig. 1) this scalar product may serve to express the orthonormalization of the mode functions ϕ_1, ϕ_2 of the outer waveguides WG1 and WG2 as well: $\langle \phi_k, \phi_j \rangle = \delta_{kj}$. Suppose the TM polarized mode ϕ_1 of waveguide WG1 with amplitude a_0 is launched into the coupling region at $z = 0$. Reflections at the input will be neglected. The power transmitted to waveguide $k = 1, 2$ at the end $z = L$ of the coupling region is given by

$$P_k(L) = |\sum_j w_{kj} \exp(-\mathrm{i}\beta_j L)|^2 \quad \text{with} \quad w_{kj} = \langle \phi_k, \chi_j \rangle \langle \chi_j, \phi_1 \rangle\,, \tag{1}$$

normalized to an input power $\beta_* |a_0|^2/(2\omega\epsilon_0) = 1$. Reflections at output are again neglected. P_1 denotes the power transfer to the input waveguide (A $\to$ B in Fig. 1).

It is a very good approximation to restrict, in (1), the sum over *all* modes to *guided* modes of the entire structure. All devices studied in this paper show only low radiation losses at input and output, $P_1(0) \geq 0.999$. We therefore prefer to calculate the propagation of fields by representing them as superpositions of guided modes.

The weights c_j allow to classify the three mode approximation mentioned above. Consider the three modes χ_-, χ_0, χ_+ with increasingly ordered propagation constants $\beta_-, \beta_0, \beta_+$ closest to β_*. Their contribution to the total power transmission is

$$\mathcal{P}_k(L) = |\sum_{j=-,0,+} w_{kj} \exp(-\mathrm{i}\beta_j L)|^2. \tag{2}$$

For the structures discussed here, $\mathcal{P}_1(0)$ turns out to be always larger than 0.9 (see Fig. 4).

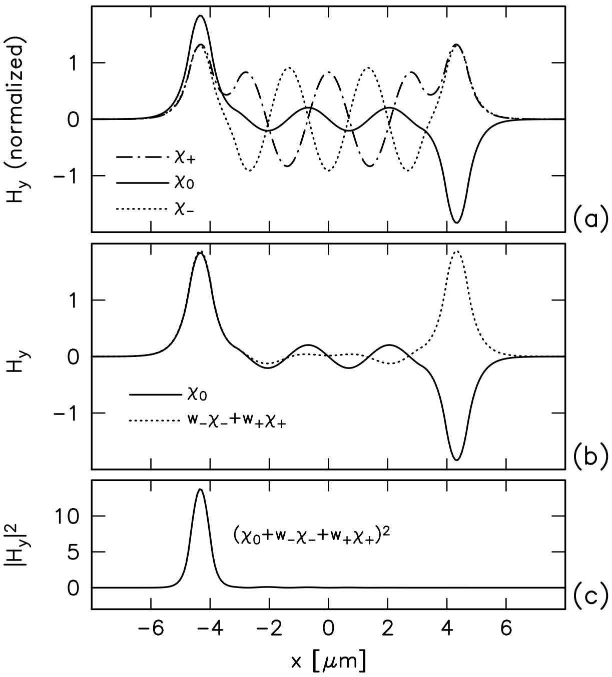

Figure 3: (a) Mode functions χ_-, χ_0, χ_+ (TM_6, TM_5, TM_4) for the structure with paramters as in Fig. 2 and $H = 6.261\mu$m. Corresponding propagation constants are $\beta_- = 10.8660/\mu$m, $\beta_0 = 10.8772/\mu$m, $\beta_+ = 10.8864/\mu$m. The linear combination of χ_- and χ_+ with weights $w_- = \sqrt{w_{1-}/w_{10}} = 0.671$ and $w_+ = \sqrt{w_{1+}/w_{10}} = 0.754$ is similar to χ_0 in the outer waveguide regions, apart from the reversed symmetry (b). The mode function of one outer waveguide can be approximated by a superposition of all three modes (c).

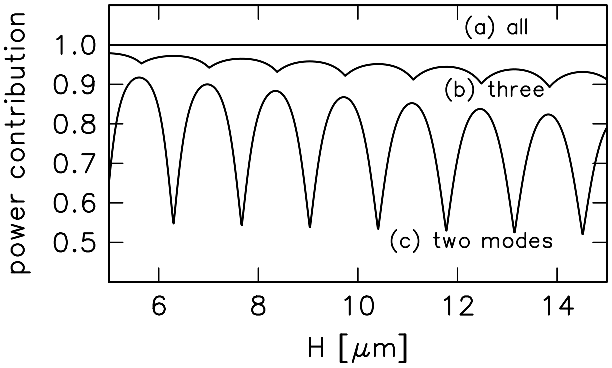

Figure 4: Contributions of different mode sets to the power transfer for zero device length versus the thickness of the central layer. (a): power transfer $P_1(0)$ of the entire mode spectrum, (b): contribution $\mathcal{P}_1(0)$ of the three most exited modes, (c): power transferred by the two most exited modes. In the neighbourhood of the maxima of curve (c) the coupling behaviour can be described approximately by the interference of two modes. Next to the maxima of curve (b) at least three modes have to be taken into account. We call these regions for H the two or three mode regime, respectively. Note that the power contribution of three modes in the three mode regime is larger than the contribution of two modes in the two mode regime.

Admittedly, the three mode approximation is somewhat crude. To obtain better results, more or all guided modes should be taken into account. However, for the purpose of finding promising points in a multidimensional parameter space, this 'three closest mode' approximation serves quite well, and we will elaborate it further.

Because of the symmetry of the entire structure and with the subsequent selection of propagation constants, χ_0 and χ_-, χ_+ have opposite parities with respect to the mirror reflection $x \to -x$. Therefore, by choosing $\phi_2(x) = \phi_1(-x)$, the scalar products within the outer waveguide modes are related by $\langle \phi_2, \chi_j \rangle = \pm \langle \phi_1, \chi_j \rangle$ for $\chi_j(x) = \pm\chi_j(-x)$. If the three modes are supposed to represent the outer waveguide modes exactly, i.e. if $\mathcal{P}_1(0) = 1$, $\mathcal{P}_2(0) = 0$, their mode weights satisfy the equations $w_{10} + w_{1-} + w_{1+} = 1$ and $w_{10} = w_{1-} + w_{1+}$.

If β_0 is closer to β_- than to β_+, define

$$\Delta\beta = \beta_0 - \beta_-, \quad \gamma = (\beta_+ - \beta_0 - \Delta\beta)/\Delta\beta, \quad r = w_{1-}/w_{10} \tag{3}$$

and

$$\Delta\beta = \beta_+ - \beta_0, \quad \gamma = (\beta_0 - \beta_- - \Delta\beta)/\Delta\beta, \quad r = w_{1+}/w_{10}$$

otherwise. $\Delta\beta$ denotes the smallest difference between the propagation constants of neighbouring modes. It defines a characteristic coupling length $L_c = \pi/\Delta\beta$. Additionally one amplitude ratio r and the asymmetry parameter γ are sufficient to characterize the power contained in the input waveguide, as we shall see.

With the above definitions the power transfer function $\mathcal{P}_1$ reads

$$\mathcal{P}_1(L) = \frac{1}{4}|1 + r\exp(\mathrm{i}\pi L/L_c) + (1-r)\exp(-\mathrm{i}(1+\gamma)\pi L/L_c)|^2. \tag{4}$$

Obviously, the conditions for the transmission to be complete — $\mathcal{P}_1(L) = 1$ — are

$$L = 2mL_c \quad \text{and} \quad \gamma = j/m. \tag{5}$$

Likewise the transmission vanishes — $\mathcal{P}_1(L) = 0$ — if

$$L = (2m+1)L_c \quad \text{and} \quad \gamma = 2j/(2m+1) \tag{6}$$

hold. In both cases m and j must be nonnegative integer numbers. Recall that (5) and (6) refer to the 'three closest modes' approximation. Parameters determined in this manner may serve as starting values for an optimization procedure which takes all modes into account.

The transferred power is minimal or maximal if the device length is an odd or even multiple of L_c, respectively. In contrast to the superposition of only two modes, the propagation constants must additionally satisfy the conditions (5) and (6) with γ as given by (3). Defining the usual coupling length L_c makes sense for three mode interference, even for nonequidistant propagation constants ($\gamma \neq 0$).

The corresponding expressions for the two mode regime result for grossly unequally weighted modes χ_-, χ_+, i.e. for $r \to 1$. In this case the conditions (5) and (6) loose their significance, and maximum or minimum power transfer occurs at each multiple of the coupling length. This situation was investigated in Ref. [10].

Variation of the parameter H alters both L_c and γ. In Fig. 5 we have marked points (H, L_c) where the condition (5) for total power transfer is met. These points occur rather frequently, thus justifying the continuous curve $L_c = L_c(H)$ for design considerations.

3 Magnetooptic layers

We will now assume that one or more layers have a linear magnetooptic effect. If the static magnetization is adjusted in the film plane and points perpendicular to the direction of propagation (transverse configuration, [14, 15]), the corresponding dielectric tensor ϵ is

$$\epsilon = \begin{pmatrix} n^2 & 0 & -\mathrm{i}\xi \\ 0 & n^2 & 0 \\ \mathrm{i}\xi & 0 & n^2 \end{pmatrix}. \tag{7}$$

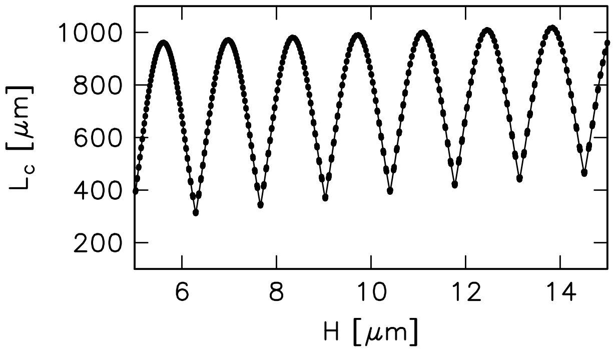

Figure 5: Coupling length L_c for different thicknesses H of the central layer. Parameters are as in Fig. 2. The line represents L_c according to (3). Regions for H with $\mathcal{P}_1(2L_c(H)) = 1$ according to the three mode approximation are marked. At such points (5) holds approximately with $m = 1$, i.e. $m\gamma(H)$ deviates from the next natural number by less than 0.1.

The off-diagonal elements are related to the specific Faraday constant θ_F by $\xi = n\lambda\theta_F/\pi$. Scalar equations for TE and TM polarized modes may be derived just as for isotropic media. In first order, ξ does not affect the propagation of TE polarized light, so our further analysis concentrates on TM modes.

It is well known that the time reversal transformation $(t, \boldsymbol{x}) \to (-t, \boldsymbol{x})$, $\rho \to \rho$, $\boldsymbol{j} \to -\boldsymbol{j}$, $\boldsymbol{E} \to \boldsymbol{E}$, $\boldsymbol{B} \to -\boldsymbol{B}$ is a symmetry of Maxwell's equations (using common notation). A wave propagating in the forward direction becomes a backward travelling wave with otherwise identical properties (reciprocity theorem). In a medium with linear magnetooptic effect, the static magnetization must change sign as well for the reciprocity theorem to hold. Since this is not the case, magnetooptic devices may exhibit nonreciprocal effects.

Our structure is mirror symmetric with respect to the $x = 0$ plane. Its transmission properties can be studied by coupling light into the first waveguide only. Likewise, reversing the sign of the imaginary nondiagonal permittivity entry iξ in all magnetooptic layers simulates reversal of the direction of propagation.

The waveguides may be investigated as multilayer structures with gyrotropic layers. Mode propagation constants and fields differ for opposite directions of propagation. These differences may be calculated by subtracting solutions for opposite ξ or by perturbation theory [16], resulting in the following expression.

Suppose the structure consists of $N + 2$ homogeneous magnetooptic layers. Then the propagation constant β related to the mode χ in the isotropic structure ($\xi = 0$) changes to $\beta + \delta\beta$:

$$\delta\beta = \frac{1}{2}\sum_{j=0}^{N}\left(\frac{\xi_{j+1}}{n_{j+1}^4} - \frac{\xi_j}{n_j^4}\right)|\chi(h_j)|^2. \tag{8}$$

h_j denotes the boundaries of the piecewise constant permittivity profile:

$$(n,\xi)(x) = \begin{cases} (n_0, \xi_0) & \text{if} \quad x < h_0 \\ (n_j, \xi_j) & \text{if} \quad h_j < x < h_{j+1} \\ (n_{N+1}, \xi_{N+1}) & \text{if} \quad h_N < x \end{cases}. \tag{9}$$

If the layers of radiatively coupled waveguides are made of magnetooptic material, usually the coupling lenghts $L_c^f = \pi/\Delta\beta_f$ for forward and $L_c^b = \pi/\Delta\beta_b$ for backward light propagation will be different. An isolator results if the device length L_{is} can be adjusted such that $L_{is} = lL_c^f = (l \pm 1)L_c^b$ holds for a positive integer number l,

$$L_{is} = \frac{\pi}{|\Delta\beta_f - \Delta\beta_b|}. \tag{10}$$

If l is even and light is injected at port A, it will leave the device at port B (see Fig. 1); if light is injected at port B, it will leave the device at port D. Likewise, if l is odd and light is injected at port A, it will leave the device at port C; if injected at C, it will leave at D.

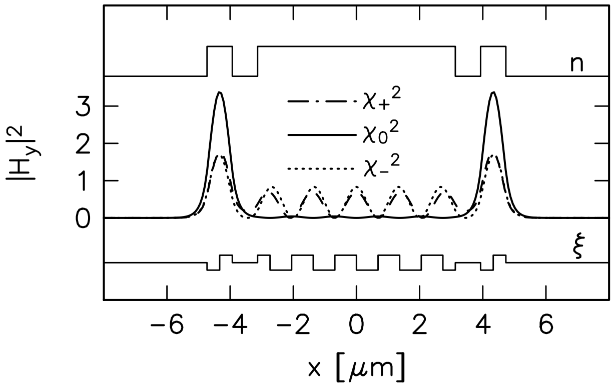

Figure 6: Absolute field values of the modes from Fig. 3. The refractive index profile is sketched above. The profile of the Faraday rotation shown below is adjusted to the shape of the mode functions to obtain optimal nonreciprocal phase shifts.

(10) defines the dependence of L_{is} on the tuning parameter H. Note that L_{is} is the length of an isolator only if $L_{is}(H)/L_c^f(H)$ turns out to be an integer. Moreover, the conditions (5) and (6) with multiplicities l and $l \pm 1$, respectively, must hold for both L_c^f and L_c^b, at least approximately. Note that (10) is unnecessarily rigid because complete power transfer is required only in forward direction.

Using the notation of section 2, (10) may be rewritten as

$$L_{is} = \frac{\pi}{2|\delta\beta_\pm - \delta\beta_0|}. \tag{11}$$

To realize a short device, a large difference between the nonreciprocal phase shift of the two most relevant modes is required. At points x with maximum difference in the absolute values of the mode fields, boundaries between regions with different Faraday rotation must be inserted (see (8)). The modes χ_0 and χ_+ or χ_-, respectively, show opposite symmetry with respect to $x = 0$. In the central layer their absolute field values are periodic in x with a period of $2d \approx \pi/\sqrt{k^2 n_3^2 - \beta_*{}^2}$. Therefore ξ should jump at $x = \pm jd$, with $j = 1, 2, \dots$, $|x| < H/2$.

If the coupling region is made of layers of thickness d with alternating Faraday rotation, the nonreciprocal phase shift $\delta\beta_0$ and $\delta\beta_+$ or $\delta\beta_-$, respectively, have a different sign. L_{is} can be further reduced if the outer waveguides are built from double magnetooptic layers as well. In this case the two layers must be ordered properly to enhance the nonreciprocal phase shift caused by the magnetic grating in the central layer. These concepts are illustrated in Fig. 6.

4 Numerical Results and Examples

The following discussion assumes two different media. A nonmagnetic medium with smaller refractive index $n_0 = n_2$ is used for the cladding and gap layers. The guiding regions are made of magnetooptic material (refractive index $n_1 = n_3$) which can be properly doped to exhibit positive and negative Faraday rotation of equal magnitude (nondiagonal elements $\pm \mathrm{i}\xi$). These assumptions are realistic, see Ref. [3].

Fig. 7 compares potential device lengthes of isolators based on radiatively coupled waveguides with identical refractive index profile. The values are estimated with the aid of (11).

If the outer waveguides are made of two layers, the total length can be shortened by a factor of 10 as compared to magnetooptic single layer outer waveguides provided that H is choosen within the three mode regime. In the case of only two relevant modes, both propagation constants are shifted in the same way because of approximately equally large amplitudes in the outer waveguides. This is the reason for the poles in curve 2 of Fig. 7. Such large variations vanish if the coupling layer is a magnetic grating. In the three mode regime, the device is half as long as compared to the double layer stuctures. It is further diminished by a factor of 3/4

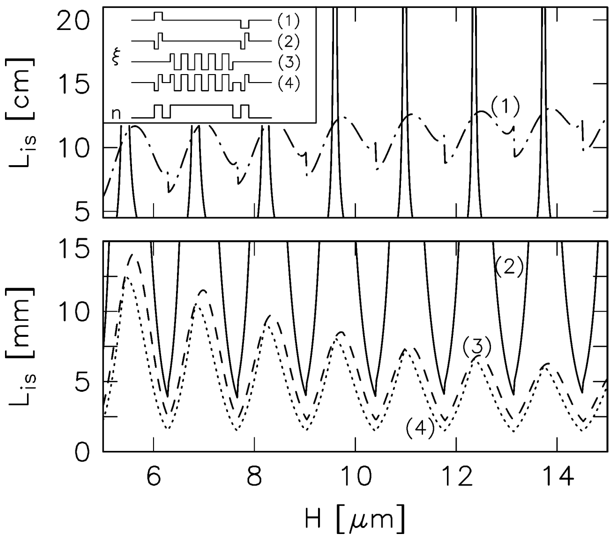

Figure 7: Isolator device length L_{is} versus the thickness H of the coupling layer. Different parts of the multilayer structures have been modeled to be magnetooptic: (1 – dash-dotted line) only the outer waveguides: single layers with opposite faraday rotation on both sides, (2 – continuous line) the outer waveguides: double layers of equal thickness with opposite Faraday rotation, (3 – dashed line) the central region: magnetic grating with alternating Faraday rotation, (4 – dotted line) the outer waveguides: double layers, additionally alternating Faraday rotation in the coupling layer. Parameters are as in Fig. 2, $|\xi| = 0.005$. Example profiles of Faraday rotation and refractive index for $H = 6.261\mu$m are sketched in the inset.

if both the central region and the outer waveguides consist of magnetooptic layers. The following paragraphs refer to such structures.

The available material ($n_0 = n_2, n_1 = n_3, \xi$), the light wavelength λ and the height h of the outer waveguides are assumed to be fixed, the gap width t and the coupler thickness H have to be optimized. We observed the following tendencies:

If t decreases, the modes of the outer waveguides deviate more and more from the modes of the entire structure which leads to larger coupling losses at input and output. If t increases, the coupling length increases in both regimes. In the three mode regime the minimal isolator length depends but weakly on t while gradients in $L_{is}(H)$ increase for larger t. We are looking for values H for which $L_c^f(H)$, $L_c^b(H)$, and $L_{is}(H)$ simultaneously have their proper meaning as coupling or isolator length. Such values occur less frequently with increasing gap width t.

For given gap width t, regions with promising thicknesses H can be selected from charts like Fig. 7. In these regions points H must be searched which guarantee a proper isolation at a device length L close to $L_{is}(H)$. These simulations must consider all guided modes of the coupler structure to give reliable results.

Larger H improves the separation of the input and output waveguides, but the number of magnetic layers, hence the structuring effort, increases. The relevant propagation constants are more closely spaced, therefore coupling lengths increase and tolerance requirements for L and H become less strict. Also, additional modes contribute to the coupling process which results in larger transmission loss due to multimode interference.

Table 1 presents three example parameter sets which correspond to well performing isolator devices. We have calculated the interference of *all* guided modes, indicated by the symbol P instead of $\mathcal{P}$ which stands for the 'three closest mode' approximation. The isolation is defined by $10 \log P_1^f / P_1^b$, the (forward transmission) loss by $-10 \log P_1^f$. Reflections at power input and output and the losses due to material absorption are neglected. The tolerance ΔX of a length parameter X is declared as follows. If all other parameters remain fixed, then $[X - \Delta X, X + \Delta X]$ is an interval of values such that isolation better that 20 dB *and* forward transmission loss below 0.5 dB are guaranteed. The parameters h and t have been varied for one of the outer waveguides only. The coupling region of structures (i), (ii), and (iii) is made up of 10, 16, and 28 layers of

	(i)	(ii)	(iii)
coupling layer thickness H [μm]	6.261	10.352	18.719
device length L [μm]	1512	1558	1504
isolation [dB]	38	55	38
forward transmission loss [db]	0.15	0.15	0.27
coupling layer tolerance ΔH [nm]	5	7	12
device length tolerance ΔL [μm]	35	40	35
gap thickness tolerance Δt [nm]	16	16	20
waveguide thickness tolerance Δh [nm]	3	3	3

Table 1: Example parameters and tolerances for isolators based on planar radiatively coupled waveguides. The remaining parameters are $\lambda = 1.3\mu$m, $h = 0.8\mu$m, $t = 0.8\mu$m, $n_0 = n_2 = 2.18$, $n_1 = n_3 = 2.30$, $|\xi| = 0.005$. See Fig. 1 for further explanations.

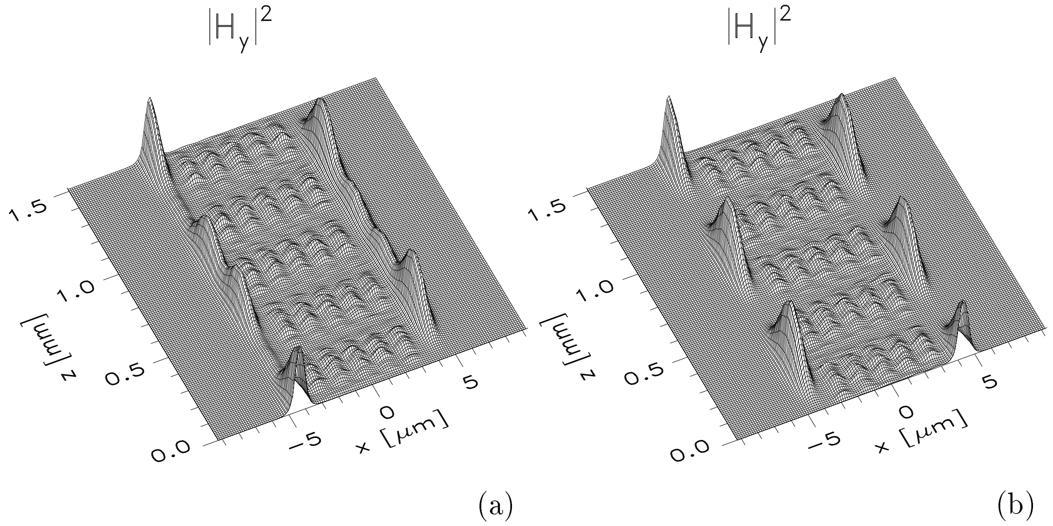

Figure 8: Light propagation in structure (i) of Tab. 1. The TM-polarized mode function of one outer waveguide is used as an initial field in $z = 0$ (a) and $z = 1.5$mm (b). In the direction of transmission the power remains in the input waveguide (a), while in the opposite direction the power is guided to the other waveguide (b). Due to $\gamma_b \approx 0$ an almost periodic interference pattern emerges in the backward direction (b).

alternating Faraday rotation. Fig. 8 illustrates light propagation in structure (i).

The three sample devices — which have been calculated and optimized with *all* guided modes — may be analyzed by the 'three closest mode' approximation as outlined in section 2. Conditions (10) and (5), (6) for good isolator performance are met, at least approximately, as demonstrated in Table 2. The ratios of device to coupling lengths should be integer numbers (4, 4, 2, 5, 3, and 3 in our case). Likewise, the asymmetry parameters γ turn out to be close to fractions of two small integers (1/2, 0, 1, 0, 2/3, and 0).

For comparison, a conventional nonreciprocal coupler (no central layer in Fig. 1) made from the same materials ($n_0 = n_2$, n_1, $|\xi|$) with the same geometry of the coupled waveguides (λ, h) must be longer than 2.75 mm. This length results for a gap width $t = 0$ and double layer waveguides. It is further enlarged by bends which are necessary for separating input and output ports. A gap width $t = 0$ corresponds to a coupling length of 11.7 μm, and a tolerance below 0.7 μm for the total device length is required. The coupling region length increases to 10.5 mm for a gap of width $2t = 0.8$ μm. Conventional coupler isolators are highly sensitive to alterations of the waveguide separation. The optimal value of 0.8 μm must be maintained with a tolerance

	(i)	(ii)	(iii)
L_c^f [μm]	381	391	739
L/L_c^f	3.97	3.98	2.04
γ^f	0.504	0.012	1.015
L_c^b [μm]	309	507	522
L/L_c^b	4.89	3.07	2.88
γ^b	0.003	0.671	0.002

Table 2: Values characterizing the coupling behaviour for the structures of table 1. The values listed here are the subject of (5), (6) and (10) for good isolator performance according to the three mode approximation. See the text for further explanation.

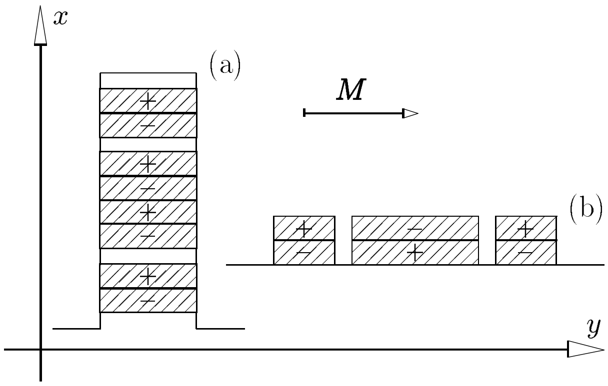

Figure 9: Concepts for isolator devices based on radiatively coupled waveguides. Cross sections perpendicular to the direction of propagation z are shown. Guiding magnetooptic layers are hatched, signs denote the signs of the Faraday rotation. Both concepts employ TM-polarized light ($|H_y| \gg |H_x|$) and the magnetization points into the direction y parallel to the substrate surface.

better than ±0.4 nm as can be estimated from the sinusoidal form of the power transfer and the dependence of the coupling length on t.

5 Rib waveguide concepts

Real integrated optical structures must guide the light in both transverse directions. Fig. 9 shows two possibilities how to exploit the advantages of radiatively coupled waveguides in three dimensions.

In (a) the multilayer structure proposed in section 3 is restricted laterally. The central strip and the second waveguide have been put onto the lower guide. To guarantee the required symmetry, the lower waveguide protrudes the substrate. In contrast to (a), structure (b) may be used as a circulator because the deviated light remains guided as well. (b) does not exploit the symmetry difference. The strongly different field amplitudes of the relevant mode functions in the coupling region and the outer waveguides cause nonreciprocal behaviour. Layers with opposite Faraday rotation would have to be realized side by side. However, it may turn out that isotropic outer waveguides in (b) allow sufficiently short devices as well.

6 Conclusions

Radiatively coupled waveguides offer an attractive alternative to the conventional two waveguide coupler. Cross-talk between the optical channels is low since they are spatially well separated. Simple conditions for complete power transfer are obtained for both the two- and the three-mode regimes. An effective circulator can be designed if the central region consists of a stack of magnetooptic layers with alternating Faraday rotation. The manufacturing of such structures requires additional technological effort, but the expected significant improvement of performance characteristics with respect to the conventional nonreciprocal coupler would well pay off.

Acknowledgments

We gratefully acknowledge financial support by Deutsche Forschungsgemeinschaft (Sonderforschungsbereich 225 and Graduiertenkolleg ”Mikrostruktur oxidischer Kristalle”).

References

[1] K. Ando. "Nonreciprocal devices for integrated optics". *Proceedings SPIE*, **1126**, 58–65, (1989).

[2] H. Dötsch, P. Hertel, B. Lührmann, S. Sure, H. P. Winkler, and M. Ye. "Applications of Magnetic Garnet Films in Integrated Optics". *IEEE Transactions on Magnetics*, **28**(5), 2979–2984, (1992).

[3] M. Wallenhorst, M. Niemöller, H. Dötsch, P. Hertel, R. Gerhardt, and B. Gather. "Enhancement of the nonreciprocal magneto-optic effect of TM modes using iron garnet double layers with opposite Faraday rotation". *Journal of Applied Physics*, **77**(7), 2902–2905, (1995).

[4] T. Mizumoto, S. Mashimo, T. Ida, and Y. Naito. "In-plane magnetized rare earth iron garnet for a waveguide optical isolator employing nonreciprocal phase shift". *IEEE Transactions on Magnetics*, **29**, 3417–3419, (1993).

[5] M. Levy, I. Ilic, R. Scarmozzino, R. M. Osgood, R. Wolfe, C. I. Guiterrez, and G. A. Prinz. "Thin-film-magnet magnetooptic waveguide isolator". *IEEE Photonics Technology Letters*, **5**, 198–200, (1994).

[6] R. Wolfe, W.-K. Wang, D. J. DiGiovanni, and A. M. Vengsarkar. "All-fiber magneto-optic isolator based on the nonreciprocal phase shift in asymmetric fiber". *Optics Letters*, **20**, 1740–1742, (1995).

[7] M. Shamonin, M. Lohmeyer, and P. Hertel. "Radiatively Coupled Magneto-Optic Waveguides". *Proceedings SPIE*, **2695**, 355–361, (1996).

[8] A. Haus and C. G. Fonstad. "Three-Waveguide Couplers for Improved Sampling and Filtering". *IEEE Journal of Quantum Electronics*, **17**(12), 2321–2325, (1981).

[9] S. M. Loktev, V. A. Sychugov, and B. A. Usievich. "Propagation of light in a system of two radiatively coupled waveguides". *Quantum Electronics*, **24**(5), 435–438, (1994).

[10] M. Shamonin, M. Lohmeyer, and P. Hertel. "Directional coupler based on radiatively coupled waveguides". *Applied Optics*, (1996), submitted for publication.

[11] J. P. Donelly. "Limitations on Power Transfer Efficiency in Three-Guide Optical Couplers". *IEEE Journal of Quantum Electronics*, **22**(5), 610–616, (1986).

[12] K. L. Chen and S. Wang. "The Crosstalk in Three-Waveguide Optical Directional Couplers". *IEEE Journal of Quantum Electronics*, **22**(7), 1039–1041, (1986).

[13] J. P. Donelly and H. A. Haus. "Symmetric Three-Guide Optical Coupler with Nonidentical Center and Outside Guides". *IEEE Journal of Quantum Electronics*, **23**(4), 401–406, (1987).

[14] A. Erdmann, M. Shamonin, P. Hertel, and H. Dötsch. "Design of nonreciprocal couplers for integrated optics". *Proceedings SPIE*, **2150**, 183–192, (1994).

[15] S. Yamamoto and T. Makimoto. "Circuit theory for a class of anisotropic and gyrotropic thin-film optical waveguides and design of non-reciprocal devices for integrated optics". *Journal of Applied Physics*, **45**, 882, (1974).

[16] M. Shamonin and P. Hertel. "Analysis of nonreciprocal phase shifters for integrated optics by the Galerkin method". *Optical Engineering*, **34**(3), 849–852, (1995).